Novel Adaptive Hierarchical Sliding Mode Control for Trajectory Tracking and Load Sway Rejection in Double-Pendulum Overhead Cranes

HUIMIN OUYANG[ID], **(Member, IEEE), JIAN WANG, GUANGMING ZHANG,**
LEI MEI, (Member, IEEE), AND XIN DENG, (Member, IEEE)
College of Electrical Engineering and Control Science, Nanjing Tech University, Nanjing 211816, China

Corresponding author: Huimin Ouyang (ouyang1982@njtech.edu.cn)

ABSTRACT Overhead cranes with double-pendulum effect seem more practical than those with single-pendulum effect. However, in this case, the dynamic performance analysis and the controller design become more difficult. Moreover, achieving both high-precision trajectory tracking and load sway rejection is a more significant issue for crane systems. For these purposes, the nonlinear dynamics of an overhead crane with double-pendulum effect is derived for the controller design. Then, a novel adaptive hierarchical sliding mode controller is presented. Unlike a traditional approach, the proposed one can make fixed sliding mode surface active to search the state trajectories. Such an adaptive design can make the states of the system to enter the desired sliding surface as soon as possible and, at the same time, can also improve the cart tracking precision. The Lyapunov technique and LaSalle's principle are employed to confirm the stability of the whole system. The experimental results validate that the proposed method has superior control performance and robustness with respect to parameter variations.

INDEX TERMS Overhead crane, double-pendulum effect, load sway rejection, tracking control, adaptive hierarchical sliding mode control.

I. INTRODUCTION

Overhead cranes are widely used in factories, mining, ports, construction sites and so on, which make industrial manufacture tend to be mechanization and automation. However, the undesired load sways caused by the motion of the cart must be suppressed, because this kind of vibration may reduce the work efficiency, cause accidence and injures people. It is important to propose a suitable controller for achieving cart tracking and load sway reduction simultaneously [1].

Until now, various control approaches have been presented for crane systems including input shaping method [2]–[10], trajectory generation method [11]–[15], tow-degree-of-freedom control approach [16]–[19], gain scheduling control [20], [21], sliding mode control [22]–[24], adaptive control [35]–[42], model predictive control methods [37]–[40], Lyapunov-based control approach [41]–[43], Fuzzy-based controller [44] and so on.

However, in many situations, the load sway reveals double-pendulum effects because of large hock mass or irregularly-shaped load. This makes the system analysis and controller design more difficult. To this end, Singhose and Kim [45], Sung and Singhose [46], Manning *et al.* [47], Vaughan *et al.* [48], and Maleki and Singhose [49] extended input shaping technology to achieve double-pendulum suppression. Masoud *et al.* [50] proposed a hybrid input shape method for double-pendulum overhead cranes. Simulations and experimental results confirmed the effectiveness of the proposed method. Huang *et al.* [51] proposed a robust command smoother for suppressing load sways in a overhead crane system with distributed-mass load. Simulations and experimental results were used to demonstrate the effectiveness of the proposed method. In addition, an S-shaped trajectory generation method was presented in [52]. Zhang *et al.* [53] presented an online motion planning approach for load sway reduction control for an overhead crane system with double-pendulum effect. Comparative simulations indicated that the proposed controller had robustness with respect to parameters variations and disturbances.

Chen *et al.* [54] proposed a time-optimal trajectory generation method considering several physical constraints for load sway suppression in double-pendulum overhead cranes. The effectiveness of the proposed approach was validated through simulations and experiments. Tuan and Lee [55] presented a hierarchical sliding mode controller for double-pendulum overhead cranes. Better control performance was obtained by comparing with a traditional sliding mode controller numerically. Zhang *et al.* [56] also presented an adaptive tracking control method for double-pendulum overhead cranes with uncertainties and disturbance. The stability of the whole control system was validated by Lyapunov-based techniques. The results indicated that the proposed controller can insure the tracking error of the cart within a given region numerically. Qian *et al.* [57] suggested a SIRMs-based fuzzy controller to suppress double-pendulum load sway in an overhead crane. Comparative simulations demonstrated the effectiveness of the proposed method. An input-shaping-based SIRMs fuzzy approach war reported in [58] for double-pendulum overhead crane. Mar *et al.* [59] presented a novel controller which is the combination of a input shaper and a feedback controller to deal with the double-pendulum problem in overhead cranes. The proposed controller had robustness with respect to disturbance and model uncertainties by simulations and experiments [59]. A nonlinear quasi-PID scheme for double-pendulum overhead cranes was introduced in [60]. Ouyang *et al.* [61] proposed a simple LMI-based robust controller for double-pendulum overhead cranes, Comparative simulations and experiments demonstrated the effectiveness of the proposed method. A nonlinear antiswing control was reported in [62]. Sun *et al.* [63] also presents an amplitude-saturated output feed-back controller for a double-pendulum overhead crane to achieve both cart positioning and load sway suppression. Experimental results confirmed that the proposed method has a better performance by compared with the exiting controllers. Although input shaping and its improved technology or other trajectory generation method have been used to solve the double pendulum effect in crane systems and achieved good results, as a typical open-loop control method, it mainly depended on the linear model of the system and only focused on the suppression control of the load sways, ignoring the positioning accuracy and speed of the cart. Moreover, the control performance might be deteriorated when parameter variations or external disturbance occurred. On the other hand, most of the closed-loop control methods, such as those proposed in [55]–[63], can provide robust or adaptive control for crane systems to improve their control performance. However, there are some problems such as lager overshoot or longer response time, since the damping ratio of the closed-loop system in the aforementioned method was a constant, which has certain 'passivity'. Hence, a control system with an active damping ratio is proposed in this paper.

To this end, the nonlinear dynamics of an overhead crane with double-pendulum effect is derived for controller design. Then, a novel adaptive hierarchical sliding mode controller

is presented. Unlike a traditional approach, the proposed one can make fixed sliding mode surface active to search the state trajectories. The stability of the whole system is confirmed by Lyapunov technique and LaSalle's principle. The effectiveness of the proposed method is demonstrated by experimental results.

In summary, the major contribution of this study is as follows.

1) To the best of our knowledge, the proposed method is the first adaptive hierarchical sliding mode controller for double-pendulum overhead crane system.
2) Compared with the existing methods, such a design not only enhances the coupling among all the states of the crane system, but also makes them reach the proposed sliding surface as fast as possible, and also improves the tracking accuracy of the cart.
3) Through the self-built overhead crane experimental platform, it is verified that the proposed method has better control performance than the traditional controllers, and also has a certain robustness with respect to parameter changes such as rope length and load mass.

The rest of this paper is organized as follows. Section II presents the nonlinear dynamic model of the double-pendulum overhead crane. The novel adaptive hierarchical sliding mode controller and stability analysis are presented in Section III. Experimental results are provided in Section IV. Finally, the conclusion of this paper is given in Section V.

II. MATHEMATIC MODEL FOR DOUBLE-PENDULUM OVERHEAD CRANE

In this section, the dynamics model of an overhead crane with double-pendulum effect as shown in Fig. 1 is presented. Parameters M_0, m_1 and m_2 denote the mass of the cart, hook and load, respectively. Parameters l_1 and l_2 denote the rope length and the distance between the center of mass of the hook and the center of mass of the load, respectively. θ_1 and θ_2 denote the hook sway and load sway angles, respectively.
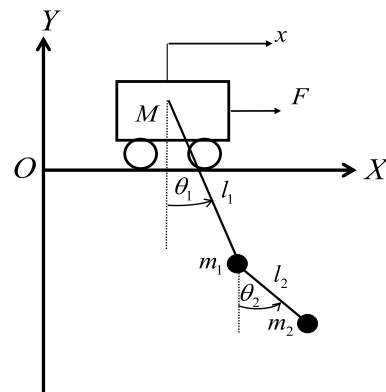

FIGURE 1. Dynamic model of overhead crane with double-pendulum effect.

By using the Lagrange's equation of motion, the nonlinear dynamics of an overhead crane is [52]–[64]

$$
\begin{aligned}
(M_0 + m_1 + m_2)\ddot{x} &+ (m_1 + m_2)l_1 \cos\theta_1 \ddot{\theta}_1 + m_2 l_2 \\
&\times \cos\theta_2 \ddot{\theta}_2 - (m_1 + m_2)l_1 \sin\theta_1 \dot{\theta}_1^2 \\
&- m_2 l_2 \sin\theta_2 \dot{\theta}_2^2 = F - f
\end{aligned} \tag{1}
$$

$$
\begin{aligned}
(m_1 + m_2)l_1 \cos\theta_1 \ddot{x} &+ (m_1 + m_2)l_1^2 \ddot{\theta}_1 + m_2 l_1 l_2 \\
&\times \cos(\theta_1 - \theta_2)\ddot{\theta}_2 + m_2 l_1 l_2 \sin(\theta_1 - \theta_2)\dot{\theta}_2^2 \\
&+ (m_1 + m_2)gl_1 \sin\theta_1 = 0
\end{aligned} \tag{2}
$$

$$
\begin{aligned}
m_2 l_2 \cos\theta_2 \ddot{x} &+ m_2 l_1 l_2 \cos(\theta_1 - \theta_2)\ddot{\theta}_1 + m_2 l_2^2 \ddot{\theta}_2 \\
&- m_2 l_1 l_2 \sin(\theta_1 - \theta_2)\dot{\theta}_1^2 + m_2 g l_2 \sin\theta_2 = 0
\end{aligned} \tag{3}
$$

where g, F and f are the gravitational acceleration, the driving force for the cart and the fiction force, respectively.

Then, the following formulation, which was obtained by the modeling technique reported in [15], was used to compensate for the friction term in the cart driven system:

$$
f = f_1 \tanh\left(\frac{\dot{x}}{\epsilon}\right) + f_2 |\dot{x}|\dot{x} \tag{4}
$$

where f_1, f_2, and ϵ are the friction related parameters, which are 4.4, -0.5 and 0.01 by off-line experiments and data fitting, respectively.

Rearrange Eps (1)-(3) in the form of a matrix, and the three equations can be rewritten as,

$$
M\ddot{q} + C\dot{q} + G = \tau
$$

$$
M = \begin{bmatrix} m_{11} & m_{12} & m_{13} \\ m_{21} & m_{22} & m_{23} \\ m_{31} & m_{32} & m_{33} \end{bmatrix}, \quad C = \begin{bmatrix} c_{11} & c_{12} & c_{13} \\ c_{21} & c_{22} & c_{23} \\ c_{31} & c_{32} & c_{33} \end{bmatrix},
$$

$$
G = \begin{bmatrix} g_1 \\ g_2 \\ g_3 \end{bmatrix}, \quad \tau = \begin{bmatrix} F \\ 0 \\ 0 \end{bmatrix}, \quad q = \begin{bmatrix} x \\ \theta_1 \\ \theta_2 \end{bmatrix}
$$

$$
m_{11} = M_0 + m_1 + m_2, \quad m_{12} = (m_1 + m_2)l_1 \cos\theta_1,
$$
$$
m_{13} = m_2 l_2 \cos\theta_2, \quad m_{21} = m_{12}, \quad m_{22} = (m_1 + m_2)l_1^2,
$$
$$
m_{23} = m_2 l_1 l_2 \cos(\theta_1 - \theta_2), \quad m_{31} = m_{13},
$$
$$
m_{32} = m_2 l_1 l_2 \cos(\theta_1 - \theta_2), \quad m_{33} = m_2 l_2^2
$$
$$
c_{11} = 0, c_{12} = -(m_1 + m_2)l_1 \sin\theta_1 \dot{\theta}_1,
$$
$$
c_{13} = -m_2 l_2 \sin\theta_2 \dot{\theta}_2, \quad c_{21} = 0, \quad c_{22} = 0,
$$
$$
c_{23} = m_2 l_1 l_2 \sin(\theta_1 - \theta_2)\dot{\theta}_2, \quad c_{31} = 0,
$$
$$
c_{32} = -m_2 l_1 l_2 \sin(\theta_1 - \theta_2)\dot{\theta}_1, \quad c_{33} = 0
$$
$$
g_1 = 0, \quad g_2 = (m_1 + m_2)gl_1 \sin\theta_1, \quad g_3 = m_2 g l_2 \sin\theta_2 \tag{5}
$$

where M, C, G, τ and q are the inertia matrix, Coriolis and centrifugal forces matrix, gravitational term vector, generalized force vector and generalized coordinates vector, respectively.

In order to design a suitable controller, the following dynamic model can be deduced from Eq. (5) with some

mathematical operation [64]:

$$
\begin{cases}
\dot{x}_1 = \dot{x} \\
\dot{x}_2 = b_1 u + d_1 \\
\dot{x}_3 = \dot{\theta}_1 \\
\dot{x}_4 = b_2 u + d_2 \\
\dot{x}_5 = \dot{\theta}_2 \\
\dot{x}_6 = b_3 u + d_3
\end{cases} \tag{6}
$$

where u is the control input of the system. The detail of terms b_1, b_2, b_3, d_1, d_2 and d_3 are included in Appendix.

III. CONTROLLER DESIGN AND STABILITY ANALYSIS
A. ADAPTIVE HIERARCHICAL SLIDING MODE CONTROLLER

In this section, a novel adaptive hierarchical sliding mode controller (AHSMC) is suggested to achieve load sway suppression and high precision cart tracking control in double-pendulum overhead cranes. Unlike a traditional one, the proposed one can make fixed sliding mode surface active to search the state trajectories. Such an adaptive design can make all the states of the system enter the desired sliding surface as soon as possible, at the same time, can also improve the cart tracking precision. The proposed sliding mode surface has three layers which covers all the state variables and their first order time derivatives.

Based on the crane mode in Eq. (6), the first layer of the sliding mode surface and its time derivative can be suggested as follows:

$$
\begin{aligned}
s_1 &= e + \lambda_1 \theta_1 \\
e &= x - x_d
\end{aligned} \tag{7}
$$
$$
\begin{aligned}
\dot{s}_1 &= \dot{e} + \lambda_1 \dot{\theta}_1 \\
\dot{e} &= \dot{x} - \dot{x}_d
\end{aligned} \tag{8}
$$

where λ_1 is a positive constant, and x_d and $\dot{x}_d$ are the desired position and velocity trajectories of the cart.

Next, combining with the state θ_2 to construct the second layer of the sliding mode surface and its time derivative, we have,

$$
s_2 = s_1 + \lambda_2 \theta_2 \tag{9}
$$
$$
\dot{s}_2 = \dot{s}_1 + \lambda_2 \dot{\theta}_2 \tag{10}
$$

where λ_2 is also a positive constant.

Because the first and second layers of the presented sliding mode surface are the linear combination of the state variables in nature, therefore, the third layer of sliding mode surface is constructed as follows:

$$
s = \dot{s}_2 + \lambda_3 s_2 \tag{11}
$$

where λ_3 is a time-varying parameter and it can be positive or negative. Hence, the estimation value of λ_3, $\hat{\lambda}_3$, is used for controller design.

Then, on the basis of the proposed sliding surface, the following controller and the adaptive law are designed:

$$u = -\frac{\hat{\lambda}_3(\dot{e} + \lambda_1\dot{\theta}_1 + \lambda_2\dot{\theta}_2)}{b_1 + \lambda_1 b_2 + \lambda_2 b_3} - \frac{\kappa s + \eta\,\mathrm{sgn}(s)}{b_1 + \lambda_1 b_2 + \lambda_2 b_3} \quad (12)$$

$$\dot{\hat{\lambda}}_3 = -\frac{s_2(d_1 + \lambda_1 d_2 + \lambda_2 d_3 - \ddot{x}_d)}{|s_2|^2 + \delta} \quad (13)$$

where κ, η and δ are positive constants to make sure that the crane control system is stable.

In order to reduce the chattering effect, the hyperbolic tangent function is used to replace the signum function. Therefore, we have,

$$u = -\frac{\hat{\lambda}_3(\dot{e} + \lambda_1\dot{\theta}_1 + \lambda_2\dot{\theta}_2)}{b_1 + \lambda_1 b_2 + \lambda_2 b_3} - \frac{\kappa s + \eta\tanh(s)}{b_1 + \lambda_1 b_2 + \lambda_2 b_3} \quad (14)$$

B. STABILITY ANALYSIS

The following Lyapunov function candidate is consider:

$$V = \frac{1}{2}s^T s \quad (15)$$

Taking time derivative of Eq. (15), we have,

$$\begin{aligned}
\dot{V} &= s^T\left(\dot{\hat{\lambda}}_3 s_2 + \lambda_3\dot{s}_2 + \ddot{s}_2\right) \\
&= s^T\left(\dot{\hat{\lambda}}_3(e + \lambda_1\theta_1 + \lambda_2\theta_2) + \hat{\lambda}_3(\dot{e} + \lambda_1\dot{\theta}_1 + \lambda_2\dot{\theta}_2)\right. \\
&\quad \left. + d_1 + \lambda_1 d_2 + \lambda_2 d_3 - \ddot{x}_d + (b_1 + \lambda_1 b_2 + \lambda_2 b_3)u\right) \quad (16)
\end{aligned}$$

Substituting Eq. (12) into Eq. (16) and according to Eq. (13), we have,

$$\dot{V} = s^T\left(-\kappa s - \eta\,\mathrm{sgn}(s)\right) < 0 \quad (17)$$

Because $V > 0$ and $\dot{V} < 0$ are satisfied, the closed-loop system is asymptotically stable at the third layer of the proposed sliding surface in the Lyapunov sense.

Moreover, the stability of the first and second layers of the proposed sliding surface should be also proven.

Firstly, because the formulation $\dot{V} < 0$ is confirmed before, a invariant and compact set Φ is considered:

$$\Phi = \left\{s \,|\, \dot{V} = 0\right\} \quad (18)$$

According to Eq. (18), we have,

$$\begin{aligned}
\Phi &= \left\{s \,|\, s = 0 \cap \dot{s} = 0\right\} \\
&= \left\{s_2 \,|\, \dot{s}_2 + \lambda_3 s_2 = 0 \cap \dot{\hat{\lambda}}_3 s_2 + \lambda_3\dot{s}_2 + \ddot{s}_2 = 0\right\} \\
&= \left\{s_2 \,|\, s_2 = \dot{s}_2 = \ddot{s}_2 = 0\right\} \quad (19)
\end{aligned}$$

It is indicated that the set Φ is attracting and contains no sets other than the coordinate origin constructed by s_2 and $\dot{s}_2$. Hence, the sliding surface s_2 is asymptotically stable by the Lassalle's principle, when $t \to \infty$.

Next, from Eq. (19), the following equation can be derived:

$$\begin{aligned}
\Phi_1 &= \left\{s_2 \,|\, s_2 = 0 \cap \dot{s}_2 = 0\right\} \\
&= \left\{s_1 \,|\, \dot{s}_1 + \lambda_2\theta_2 = 0 \cap \dot{s}_1 + \lambda_2\dot{\theta}_2 = 0\right\} \\
&= \left\{s_1 \,|\, s_1 = \dot{s}_1 = \ddot{s}_1 = 0\right\} \quad (20)
\end{aligned}$$

Using the similar manner, the sling mode surface s_1 is also asymptotically stable, when $t \to \infty$.

From Eqs. (19) and (20), the limits of s_2, $\dot{s}_2$, s_1 and $\dot{s}_1$ are,

$$\lim_{t\to\infty} s_2 = \lim_{t\to\infty}(s_1 + \lambda_2\theta_2) = 0 \quad (21)$$

$$\lim_{t\to\infty} \dot{s}_2 = \lim_{t\to\infty}(\dot{s}_1 + \lambda_2\dot{\theta}_2) = 0 \quad (22)$$

$$\lim_{t\to\infty} s_1 = \lim_{t\to\infty}(e + \lambda_1\theta_1) = 0 \quad (23)$$

$$\lim_{t\to\infty} \dot{s}_1 = \lim_{t\to\infty}(\dot{e} + \lambda_1\dot{\theta}_1) = 0 \quad (24)$$

According to Eqs. (21)-(24), we have

$$\lim_{t\to\infty} \theta_2 = 0 \quad (25)$$

$$\lim_{t\to\infty} \dot{\theta}_2 = 0 \quad (26)$$

$$\lim_{t\to\infty} e = -\lim_{t\to\infty}\lambda_1\theta_1 = \text{constant} \quad (27)$$

$$\lim_{t\to\infty} \dot{e} = -\lim_{t\to\infty}\lambda_1\dot{\theta}_1 = \text{constant} \quad (28)$$

Further, due to the existence of gravity, the state variable θ_1 always reach 0 when $t \to \infty$ from physical point of view [55]. Therefore, $\lim_{t\to\infty}\theta_1 = 0$, $\lim_{t\to\infty}\dot{\theta}_1 = 0$, $\lim_{t\to\infty} e = 0$ and $\lim_{t\to\infty}\dot{e} = 0$ are satisfied.

IV. RESULTS AND DISCUSSION

A. REFERENCE TRAJECTORY FOR CART MOTION

In order to evaluate the control performance of the proposed controller, a cycloid-like motion trajectory was applied to the crane system [16]:

$$x_d = (x_f - x_0)\left\{\frac{t}{t_s} - \frac{1}{2\pi}\sin\left(2\pi\frac{t}{t_s}\right)\right\} + x_0 \quad (29)$$

where x_f, x_0, t_s and t_f denote the final position, the initial position, the settling time and the final time. We set $x_0 = 0$[m], $x_f = 0.5$[m], and $t_s = 3$[s]. Meanwhile, x_d is set as $x_d = x_f$ for $t \in (t_s, t_f]$, and $t_f = 10$[s]. We use this kind of curve as the reference trajectory because other trajectories such as traditional step one or input shaped one has discontinuous characteristics or depends on the crane model.

B. EXPERIMENTAL SYSTEM

The self-built test bed in [61] was used to confirm the control performance of the proposed method. As shown in Fig.2, the main parts of the equipment consists of four Panasonic motors, a boom, a trolley, a hook and a load. In this study, the cart-hook-load system, which can be seen as an overhead
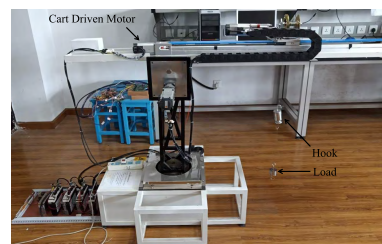

FIGURE 2. Experimental system.

crane with double-pendulum effect was used for experimental verifications. At the same time, the load sway angles were measured by the sensor systems shown in Fig. 3.
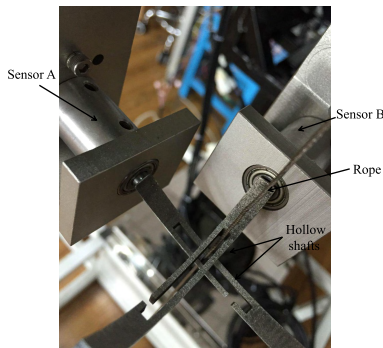

FIGURE 3. Sensor system for the first stage load sway.

In the control system of the experimental setup, a Googoltech motion control board (GT-400-SV-PCI) is employed to obtain information from the encoders, at the same time, a desired force is calculated by the DSP which is integrated in the motion control board. Then a voltage command is generated by a D/A converter to drive the servo motor. The MATLAB/Simulink real-time windows target operated in Windows XP is used for control algorithm implementation, with the control period being set as 0.005s.

C. EXPERIMENTAL RESULTS

In this section, we conducted numerous experiments to demonstrate the effectiveness of the proposed method. The parameters of the crane system and controller gains which were obtained by a trial and error method used in these experiments are given in Tab. 1 and Tab. 2.

TABLE 1. Physical parameters of overhead crane system.

M_0[kg]	6.50	m_1[kg]	2.00	m_2[kg]	0.60
l_1[m]	0.50	l_2[m]	0.40	g[m/s^2]	9.80

TABLE 2. Proposed controller gains.

λ_1	0.03	λ_2	0.05	κ	50.00
η	0.03	δ	0.50	–	–

Firstly, the proposed controller was compared with two traditional methods which are a conventional sliding mode control (CSMC) reported in [55], a linear state feedback control (LSFC) and a LMI-based controller in [61]. More precisely, the CSMC is presented as follows:

$$u = -(m_1 + m_2)l_1 \cos\theta_1\ddot{\theta}_1 - m_2l_2 \cos\theta_2\ddot{\theta}_2$$
$$+ (m_1 + m_2)l_1 \sin\theta_1\dot{\theta}_1^2 + m_2l_2 \sin\theta_2\dot{\theta}_2^2$$
$$- (M_0 + m_1 + m_2)(\lambda\dot{x} + \alpha\dot{\theta}_1 + \beta\dot{\theta}_2) - K \operatorname{sgn}(s) \quad (30)$$

where λ, α, β, and K are controller gains. After carefully tuning, these parameters were set as $\lambda = 0.5$, $\alpha = -1.22$, $\beta = -0.01$ and $K = 5$ to obtain good performance for the same crane system. In addition, s is the presented sliding mode surface in [55], and the signum function was replaced by a saturation function for reducing the chattering in the control system. On the other hand, the LSFC is formulated as follows:

$$u = -k_1(x - x_d) - k_2(\dot{x} - \dot{x}_d) - k_3\theta_1 - k_4\dot{\theta}_1 - k_5\theta_2 - k_6\dot{\theta}_2 \quad (31)$$

TABLE 3. Quantified results under condition $l_1 = 0.50$[m].

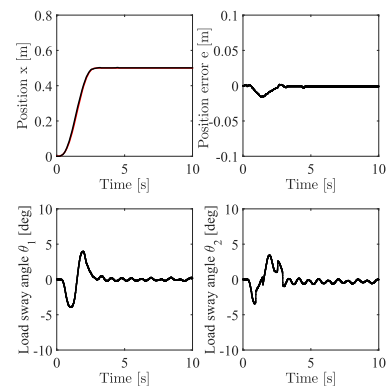| Control method	t_s[s]	e_{max}[m]
Proposed controller	2.96	0.015
CSMC	5.99	0.065
LSFC	3.77	0.035
LMI-based controller	4.62	0.112
Control method	θ_{1max}[deg]	θ_{2max}[deg]
Proposed controller	3.95	3.41
CSMC	3.55	4.23
LSFC	4.29	5.25
LMI-based controller	3.22	5.07

FIGURE 4. Experimental results by the AHSMC with $l_1 = 0.5$[m].

where k_1, k_2, k_3, k_4, k_5 and k_6 are gains, which were set as $k_1 = 600.71$, $k_2 = 269.32$, $k_3 = -128.86$, $k_4 = 86.54$, $k_5 = -153.48$ and $k_6 = -16.82$ by a pole placement method. The results obtained by the three controllers are shown in Fig.4-7. It is noted that the position error e is defined as $e = x_d - x$ in these figures. At the same time, the quantitative analysis, which includes the settling time t_s, the maximum value of tracking error e_{max}, the maximum value of hook sway angle θ_{1max} and the maximum value of load sway angle θ_{2max}, for these results is shown in Tab. 3. From these figures and Tab. 3, the cart trajectory tracking performance is achieved by using the four controllers. However, the cart takes the shortest time to the desired position by the proposed controller, whereas the longest time was taken by the CSMC. It is obvious that the overshoot and undershoot exist in Figs. 5-7, because the damping ratios of the closed-loop crane control system were
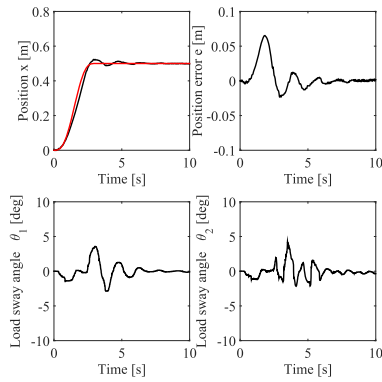
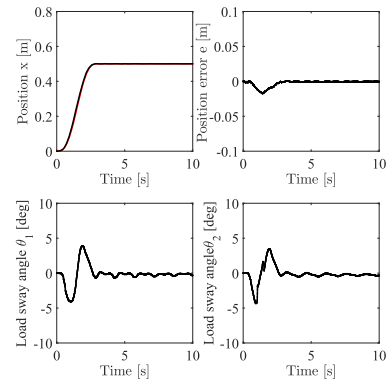**FIGURE 5.** Experimental results by the CSMC with $l_1 = 0.5$[m].

FIGURE 6. Experimental results by the LSFC with $l_1 = 0.5$[m].
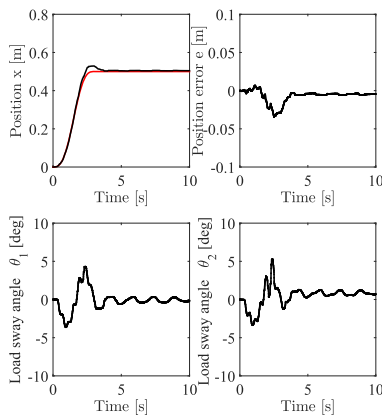

FIGURE 7. Experimental results by the LMI-based controller with $l_1 = 0.5$[m].

FIGURE 8. Experimental results with $l_1 = 0.45$[m].
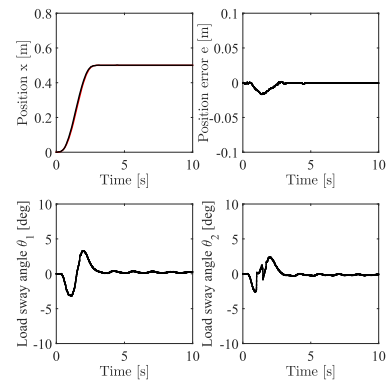

FIGURE 9. Experimental results with $l_1 = 0.55$[m].

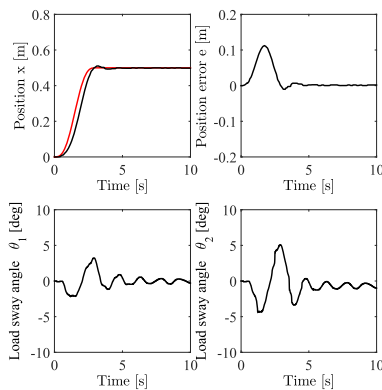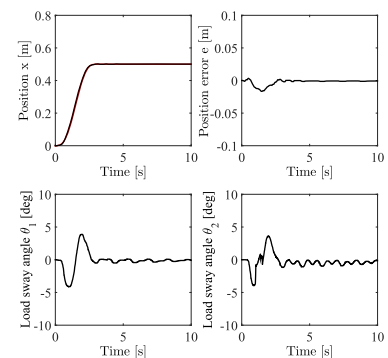**FIGURE 10.** Experimental results $m_2 = 0.55$[kg].

set as a constant. At the same time, the maximum value of the tracking error e_{max} can be reduced about 57%, 77%, and 87% comparing with the results obtained by the LSFC, the CSMC, and the LMI-based method. On the other hand, although the double-pendulum load sways can also be decreased by the three controllers and almost converge to zero, the proposed method also provides the shortest load sways reduction time than that by the traditional approaches.

Next, in order to demonstrate the robustness performance of the proposed controller, we carried out some experiments

by changing the rope length (i.e. l_1 was set as $l_1 = 0.45$[m] or $l_1 = 0.55$[m]), the load mass (i.e. m_2 was set as $m_2 = 0.55$[kg] or $m_2 = 0.65$[kg]) and the desired position of the cart (i.e. x_d was set as $x_d = 0.4$[m] or $x_d = 0.6$[m]). These results, which include the cart motion trajectory x, the tracking error e, the hook sway angle θ_1 and the load sway angle θ_2, are shown in Figs. 8-13, respectively. By comparing the results of Fig. 4, Fig. 8 and Fig. 9, it can be found that the cart can track the desired trajectory well, and the double-pendulum load sway angles are also well suppressed. Similarly, by comparing the results of Fig. 4, Fig. 10 and Fig. 11, it can be found that the proposed method can achieve almost the same transient and steady characteristics for the
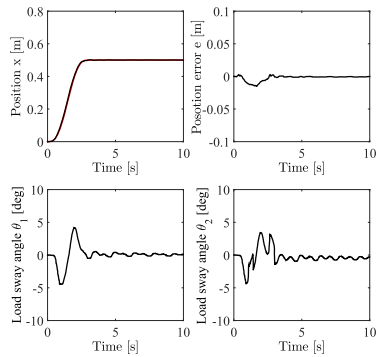
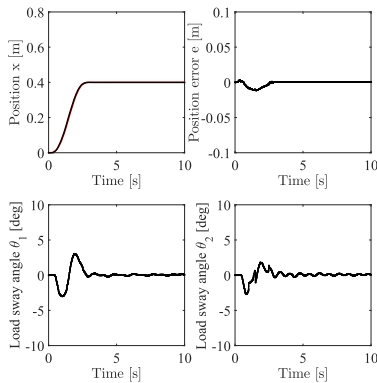**FIGURE 11.** Experimental results with $m_2 = 0.65$[kg].

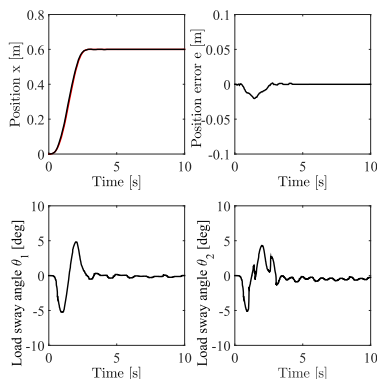**FIGURE 12.** Experimental results $x_d = 0.4$[m].

FIGURE 13. Experimental results with $x_d = 0.6$[m].

cart and load sways rejection performance even when the load mass changed. Finally, by comparing Fig. 4, Fig. 12 and Fig. 13, it can be found that the proposed method can also be applied to the crane system for different target positions of the cart. It is indicated that the proposed controller is insensitive with parameter variation, which is of great significance to practical applications.

V. CONCLUSION

In order to achieve both high-precision tracking control and load sway suppression in double-pendulum overhead cranes, the nonlinear dynamic crane model was derived.

Then, a novel adaptive hierarchical sliding mode controller, which can make all state variables of the system reach the designed sliding mode surface more quickly and accurately, was presented. Experimental results show that the trajectory tracking of the cart and double-pendulum load sway suppression were realized simultaneously by using the proposed method. At the same time, by comparing with the LSFC, the CSMC, and the LMI-based approach, it is found that the tracking error of the cart can be reduced about 57%, 77%, and 87%, respectively. In addition, the method proposed in this paper is also robust to the change of system parameters.

APPENDIX

The section brief presents the detailed information for b_1, b_2, b_3, d_1, d_2, and d_3 in Eq. (5), which are as follows:

$$b_1 = \frac{b_{11}}{\delta}, b_2 = \frac{b_{12}}{\delta}, b_3 = \frac{b_{13}}{\delta}$$

$$d_1 = \frac{d_{11}}{\delta}, d_2 = \frac{d_{12}}{\delta}, d_3 = \frac{d_{13}}{\delta}$$

$$\begin{aligned}\delta = &(m_1+m_2)m_2 l_1^2 l_2^2((M_0+m_1+m_2)-(m_1+m_2)\cos^2\theta_1)\\ &-m_2^2 l_1^2 l_2^2((m_1+m_2)\cos^2\theta_2\\ &+(M_0+m_1+m_2)\cos^2(\theta_1-\theta_2)\\ &-2(m_1+m_2)\cos\theta_1\cos\theta_2\cos(\theta_1-\theta_2)),\end{aligned}$$

$$b_{11} = (m_1+m_2)m_2 l_1^2 l_2^2 - m_2^2 l_1^2 l_2^2 \cos^2(\theta_1-\theta_2),$$

$$b_{12} = m_2^2 l_1^2 l_2^2 \cos\theta_2\cos(\theta_1-\theta_2) - (m_1+m_2)m_2 l_1 l_2^2 \cos\theta_1,$$

$$\begin{aligned}b_{13} = &(m_1+m_2)m_2 l_1^2 l_2 \cos\theta_1\cos(\theta_1-\theta_2)\\ &-(m_1+m_2)m_2 l_1^2 l_2 \cos\theta_2,\end{aligned}$$

$$\begin{aligned}d_{11} = &((m_1+m_2)m_2 l_1^2 l_2^2 - m_2^2 l_1^2 l_2^2 \cos^2(\theta_1-\theta_2))\\ &\times((m_1+m_2)l_1\dot\theta_1^2\sin\theta_1 + m_2 l_2\dot\theta_2^2\sin\theta_2)\\ &+((m_1+m_2)m_2 l_1 l_2^2\cos\theta_1 - m_2^2 l_1 l_2^2\cos\theta_2)\cos(\theta_1-\theta_2))\\ &\times(m_2 l_1 l_2\dot\theta_2^2\sin(\theta_1-\theta_2) + (m_1+m_2)gl_1\sin\theta_1)\\ &+((m_1+m_2)m_2 l_1^2 l_2\cos\theta_2 - m_2^2 l_1^2 l_2\cos\theta_1\cos(\theta_1-\theta_2))\\ &\times(-m_2 l_1 l_2\dot\theta_1^2\sin(\theta_1-\theta_2) + m_2 gl_2\sin\theta_2),\end{aligned}$$

$$\begin{aligned}d_{12} = &(m_2^2 l_1 l_2^2\cos\theta_2\cos(\theta_1-\theta_2) - (m_1+m_2)m_2 l_1 l_2^2\cos\theta_1)\\ &\times((m_1+m_2)l_1\dot\theta_1^2\sin\theta_1 + m_2 l_2\dot\theta_2^2\sin\theta_2)\\ &+(m_2^2 l_2^2\cos^2\theta_2)\\ &-(M_0+m_1+m_2)m_2 l_2^2)(m_2 l_1 l_2\dot\theta_2^2\sin(\theta_1-\theta_2)\\ &+(m_1+m_2)gl_1\sin\theta_1)\\ &+((M_0+m_1+m_2)m_2 l_1 l_2\cos(\theta_1-\theta_2)\\ &-(m_1+m_2)m_2 l_1 l_2\cos\theta_1\cos\theta_2)(-m_2 l_1 l_2\dot\theta_1^2\sin(\theta_1-\theta_2)\\ &+m_2 gl_2\sin\theta_2)\end{aligned}$$

$$\begin{aligned}d_{13} = &((m_1+m_2)m_2 l_1^2 l_2(\cos\theta_1\cos(\theta_1-\theta_2) - \cos\theta_2))\\ &\times((m_1+m_2)l_1\dot\theta_1^2\sin\theta_1 + m_2 l_2\dot\theta_2^2\sin\theta_2)\\ &+((M_0+m_1+m_2)m_2 l_1 l_2\cos(\theta_1-\theta_2) - (m_1+m_2)m_2 l_1 l_2\\ &\times\cos\theta_1\cos\theta_2)(m_2 l_1 l_2\dot\theta_2^2\sin(\theta_1-\theta_2)\\ &+(m_1+m_2)gl_1\sin\theta_1)\\ &+((m_1+m_2)^2 l_1^2\cos^2\theta_1 - (M_0+m_1+m_2)(m_1+m2)l_1^2)\\ &\times(-m_2 l_1 l_2\dot\theta_1^2\sin(\theta_1-\theta_2) + m_2 gl_2\sin\theta_2)\end{aligned}$$

REFERENCES

[1] L. Ramli, Z. Mohamed, A. M. Abdullahi, H. I. Jaafar, and I. M. Lazim, "Control strategies for crane systems: A comprehensive review," *Mech. Syst. Signal Process.*, vol. 95, pp. 1–23, Oct. 2017.

[2] L. Ramli, Z. Mohamed, and H. I. Jaafar, "A neural network-based input shaping for swing suppression of an overhead crane under payload hoisting and mass variations," *Mech. Syst. Signal Process.*, vol. 107, pp. 484–501, Jul. 2018.

[3] A. M. Abdullahi *et al.*, "Adaptive output-based command shaping for sway control of a 3D overhead crane with payload hoisting and wind disturbance," *Mech. Syst. Signal Process.*, vol. 98, pp. 157–172, Jan. 2018.

[4] J. J. Potter and W. E. Singhose, "Design and human-in-the-loop testing of reduced-modification input shapers," *IEEE Trans. Control Syst. Technol.*, vol. 24, no. 4, pp. 1513–1520, Jul. 2016.

[5] X. Xie, J. Huang, and Z. Liang, "Using continuous function to generate shaped command for vibration reduction," *Proc. Inst. Mech. Eng., I, J. Syst. Control Eng.*, vol. 227, no. 6, pp. 523–528, 2013.

[6] J. Huang, E. Maleki, and W. Singhose, "Dynamics and swing control of mobile boom cranes subject to wind disturbances," *IET Control Theory Appl.*, vol. 7, no. 9, pp. 1187–1195, Jun. 2013.

[7] H. Saeidi, M. Naraghi, and A. A. Raie, "A neural network self tuner based on input shapers behavior for anti sway system of gantry cranes," *J. Vib. Control*, vol. 19, no. 13, pp. 1936–1949, 2012.

[8] W. E. Singhose and J. Vaughan, "Reducing vibration by digital filtering and input shaping," *IEEE Trans. Control Syst. Technol.*, vol. 19, no. 6, pp. 1410–1420, Nov. 2011.

[9] E. Maleki and W. Singhose, "Dynamics and control of a small-scale boom crane," *J. Comput. Nonlinear Dyn.*, vol. 6, no. 3, pp. 031015-1–031015-8, 2011.

[10] W. Singhose, R. Eloundou, and J. Lawrence, "Command generation for flexible systems by input shaping and command smoothing," *J. Guid., Control, Dyn.*, vol. 33, no. 6, pp. 1697–1707, 2010.

[11] M. J. Maghsoudi, Z. Mohamed, A. R. Husain, and M. O. Tokhi, "An optimal performance control scheme for a 3D crane," *Mech. Syst. Signal Process.*, vols. 66–67, pp. 756–768, Jan. 2016.

[12] K. A. Alghanim, K. A. Alhazza, and Z. N. Masoud, "Discrete-time command profile for simultaneous travel and hoist maneuvers of overhead cranes," *J. Sound Vib.*, vol. 345, pp. 47–57, Jun. 2015.

[13] N. Sun and Y. Fang, "An efficient online trajectory generating method for underactuated crane systems," *Int. J. Robust Nonlinear Control*, vol. 24, pp. 1653–1663, Jul. 2014.

[14] N. Uchiyama, H. Ouyang, and S. Sano, "Simple rotary crane dynamics modeling and open-loop control for residual load sway suppression by only horizontal boom motion," *Mechatronics*, vol. 23, no. 8, pp. 1223–1236, 2013.

[15] N. Sun, Y. Fang, Y. Zhang, and B. Ma, "A novel kinematic coupling-based trajectory planning method for overhead cranes," *IEEE/ASME Trans. Mechatronics*, vol. 17, no. 1, pp. 166–173, Feb. 2012.

[16] H. Ouyang, G. Zhang, L. Mei, X. Deng, and D. Wang, "Load vibration reduction in rotary cranes using robust two-degree-of-freedom control approach," *Adv. Mech. Eng.*, vol. 8, no. 3, pp. 1–11, 2016.

[17] D. Fujioka and W. Singhose, "Input-shaped model reference control of a nonlinear time-varying double-pendulum crane," in *Proc. 10th Asian Control Conf. (ASCC)*, Kota Kinabalu, Malaysia, May/Jun. 2015, pp. 1–6.

[18] M. Z. M. Zain, M. O. Tokhi, and Z. Mohamed, "Hybrid learning control schemes with input shaping of a flexible manipulator system," *Mechatronics*, vol. 16, nos. 3–4, pp. 209–219, 2006.

[19] Z. Mohamed, J. M. Martins, M. O. Tokhi, J. Sá da Costa, and M. A. Botto, "Vibration control of a very flexible manipulator system," *Control Eng. Pract.*, vol. 13, no. 3, pp. 267–277, 2005.

[20] M. Ermidoro, A. L. Cologni, S. Formentin, and F. Previdi, "Fixed-order gain-scheduling anti-sway control of overhead bridge cranes," *Mechatronics*, vol. 39, pp. 237–247, Nov. 2016.

[21] K. Zavari, G. Pipeleers, and J. Swevers, "Gain-scheduled controller design: Illustration on an overhead crane," *IEEE Trans. Ind. Electron.*, vol. 61, no. 7, pp. 3713–3718, Jul. 2014.

[22] D. Chwa, "Sliding-mode-control-based robust finite-time antisway tracking control of 3-D overhead cranes," *IEEE Trans. Ind. Electron.*, vol. 64, no. 8, pp. 6775–6784, Aug. 2017.

[23] L. A. Tuan, S.-G. Lee, D. H. Ko, and L. C. Nho, "Combined control with sliding mode and partial feedback linearization for 3D overhead cranes," *Int. J. Robust Nonlinear Control*, vol. 24, no. 18, pp. 3372–3386, 2014.

[24] Q. H. Ngo and K. S. Hong, "Sliding-mode antisway control of an offshore container crane," *IEEE/ASME Trans. Mechtronics*, vol. 17, no. 2, pp. 201–209, Apr. 2012.

[25] M. Zhang, X. Ma, X. Rong, R. Song, X. Tian, and Y. Li, "A partially saturated adaptive learning controller for overhead cranes with payload hoisting/lowering and unknown parameters," *Nonlinear Dyn.*, vol. 89, no. 3, pp. 1779–1791, 2017.

[26] N. Sun, Y. Fang, H. Chen, and B. He, "Adaptive nonlinear crane control with load hoisting/lowering and unknown parameters: Design and experiments," *IEEE/ASME Trans. Mechatronics*, vol. 20, no. 5, pp. 2107–2119, Oct. 2015.

[27] Y.-F. Chen and A.-C. Huang, "Adaptive control of rotary inverted pendulum system with time-varying uncertainties," *Nonlinear Dyn.*, vol. 76, no. 1, pp. 95–102, 2014.

[28] W. He, S. Zhang, and S. S. Ge, "Adaptive control of a flexible crane system with the boundary output constraint," *IEEE Trans. Ind. Electron.*, vol. 61, no. 8, pp. 4126–4133, Aug. 2014.

[29] Q. H. Ngo and K. S. Hong, "Adaptive sliding mode control of container cranes," *IET Control Theory Appl.*, vol. 6, no. 5, pp. 662–668, 2013.

[30] C. Li, Z. Ding, J. Yi, Y. Lv, and G. Zhang, "Deep belief network based hybrid model for building energy consumption prediction," *Energies*, vol. 11, no. 1, p. 242, 2017, doi: 10.3390/en11010242.

[31] C. Li, J. Yi, H. Wang, G. Zhang, and J. Li, "Interval data driven construction of shadowed sets with application to linguistic word modelling," *Inf. Sci.*, to be published, doi: 10.1016/j.ins.2018.11.018.

[32] D. Qian, C. Li, S. Lee, and C. Ma, "Robust formation maneuvers through sliding mode for multi-agent systems with uncertainties," *IEEE/CAA J. Autom. Sinica*, vol. 5, no. 1, pp. 342–351, Jan. 2018.

[33] D. Qian, S. Tong, J. Guo, and S. Lee, "Leader-follower-based formation control of nonholonomic mobile robots with mismatched uncertainties via integral sliding mode," *Proc. Inst. Mech. Eng., I, J. Syst. Control Eng.*, vol. 229, no. 6, pp. 559–569, 2015.

[34] D. Qian, S. Tong, H. Liu, and X. Liu, "Load frequency control by neural-network-based integral sliding mode for nonlinear power systems with wind turbines," *Neurocomputing*, vol. 173, pp. 875–885, Jan. 2016.

[35] Y. Fang, B. Ma, P. Wang, and X. Zhang, "A motion planning-based adaptive control method for an underactuated crane system," *IEEE Trans. Control Syst. Technol.*, vol. 20, no. 1, pp. 241–248, Jan. 2012.

[36] J. Kalmari, J. Backman, and A. Visala, "Nonlinear model predictive control of hydraulic forestry crane with automatic sway damping," *Comput. Electron. Agricult.*, vol. 109, pp. 36–45, Nov. 2014.

[37] J. Smoczek and J. Szpytko, "Particle swarm optimization-based multivariable generalized predictive control for an overhead crane," *IEEE/ASME Trans. Mechatron.*, vol. 22, no. 1, pp. 258–268, Feb. 2017.

[38] H. Chen, Y. Fang, and N. Sun, "A swing constraint guaranteed MPC algorithm for underactuated overhead cranes," *IEEE/ASME Trans. Mechatronics*, vol. 21, no. 5, pp. 2543–2555, Oct. 2016.

[39] Z. Wu, X. Xia, and B. Zhu, "Model predictive control for improving operational efficiency of overhead cranes," *Nonlinear Dyn.*, vol. 79, no. 4, pp. 2639–2657, 2015.

[40] D. Jolevski and O. Bego "Model predictive control of gantry/bridge crane with anti-sway algorithm," *J. Mech. Sci. Technol.*, vol. 29, no. 2, pp. 827–834, 2015.

[41] N. Sun, Y. Fang, H. Chen, Y. Fu, and B. Lu, "Nonlinear stabilizing control for ship-mounted cranes with ship roll and heave movements: Design, analysis, and experiments," *IEEE Trans. Syst., Man, Cybern. Syst.*, vol. 48, no. 10, pp. 1781–1793, Oct. 2018.

[42] M. Zhang, X. Ma, X. Rong, R. Song, X. Tian, and Y. Li, "An enhanced coupling nonlinear tracking controller for underactuated 3D overhead crane systems," *Asian J. Control*, vol. 20, no. 5, pp. 1839–1854, 2018.

[43] N. Sun, T. Yang, H. Chen, Y. Fang, and Y. Qian, "Adfor 4-DOF rotary cranes subject to uncertain/unknown parameters with hardware experiments," *IEEE Trans. Syst., Man, Cybern. Syst.*, to be published, doi: 10.1109/TSMC.2017.2765183.

[44] Y.-G. Sun, H.-Y. Qiang, J.-Q. Xu, and D.-S. Dong, "The nonlinear dynamics and anti-sway tracking control for offshore container crane on a mobile harbor," *J. Marine Sci. Technol.*, vol. 25, no. 6, pp. 656–665, 2012.

[45] W. Singhose, D. Kim, and M. Kenison, "Input shaping control of double-pendulum bridge crane oscillations," *J. Dyn. Syst., Meas., Control*, vol. 130, no. 3, pp. 034504-1–034504-7, 2008.

[46] Y. G. Sung and W. E. Singhose, "Robustness analysis of input shaping commands for two-mode flexible systems," *IET Control Theory Appl.*, vol. 3, no. 6, pp. 722–730, Jun. 2009.

[47] R. Manning, J. Clement, D. Kim, and W. Singhose, "Dynamics and control of bridge cranes transporting distributed-mass payloads," *J. Dyn. Syst., Meas., Control*, vol. 132, no. 1, pp. 014505-1–014505-8, 2010.

[48] J. Vaughan, D. Kim, and W. Singhose, "Control of tower cranes with double-pendulum payload dynamics," *IEEE Trans. Control Syst. Technol.*, vol. 18, no. 6, pp. 1345–1358, Nov. 2010.

[49] E. Maleki and W. Singhose, "Swing dynamics and input-shaping control of human-operated double-pendulum boom cranes," *J. Comput. Nonlinear Dyn.*, vol. 7, no. 3, pp. 031006-1–031006-10, 2012.

[50] Z. Masoud, K. Alhazza, E. Abu-Nada, and M. Majeed, "A hybrid command-shaper for double-pendulum overhead cranes," *J. Vib. Control*, vol. 20, no. 1, pp. 24–37, 2012.

[51] J. Huang, X. Xie, and Z. Liang, "Control of bridge cranes with distributed-mass payload dynamics," *IEEE/ASME Trans. Mechatronics*, vol. 20, no. 1, pp. 481–486, Feb. 2015.

[52] H. Ouyang, J. Hu, G. Zhang, L. Mei, and X. Deng, "Decoupled linear model and S-shaped curve motion trajectory for load sway reduction control in overhead cranes with double-pendulum effect," *Proc. Inst. Mech. Eng., C, J. Mech. Eng. Sci.*, 2018, doi: 10.1177/0954406218819029.

[53] M. Zhang, X. Ma, H. Chai, X. Rong, X. Tian, and Y. Li, "A novel online motion planning method for double-pendulum overhead cranes," *Nonlinear Dyn.*, vol. 85, no. 2, pp. 1079–1090, 2016.

[54] H. Chen, Y.-C. Fang, N. Sun, and Y.-Z. Qian, "Pseudospectral method based time optimal anti-swing trajectory planning for double pendulum crane systems," (in Chinese), *Acta Automat Sinica*, vol. 42, no. 1, pp. 153–160, 2016.

[55] L. A. Tuan and S.-G. Lee, "Sliding mode controls of double-pendulum crane systems," *J. Mech. Sci. Technol.*, vol. 27, no. 6, pp. 1863–1873, 2013.

[56] M. Zhang, X. Ma, X. Rong, X. Tian, and Y. Li, "Adaptive tracking control for double-pendulum overhead cranes subject to tracking error limitation, parametric uncertainties and external disturbances," *Mech. Syst. Signal Process.*, vols. 76–77, pp. 15–32, Aug. 2016.

[57] D. Qian, S. Tong, and S. Lee, "Fuzzy-Logic-based control of payloads subjected to double-pendulum motion in overhead cranes," *Automat Constr*, vol. 65, pp. 133–143, Mar. 2016.

[58] D. Qian, S. Tong, B. Yang, and S. Lee, "Design of simultaneous input-shaping-based SIRMs fuzzy control for double-pendulum-type overhead cranes," *Bull. Polish Acad. Sci. Tech. Sci.*, vol. 63, no. 4, pp. 887–896, 2015.

[59] R. Mar, A. Goyal, V. Nguyen, T. Yang, and W. Singhose, "Combined input shaping and feedback control for double-pendulum systems," *Mech. Syst. Signal Process.*, vol. 85, pp. 267–277, Feb. 2017.

[60] N. Sun, T. Yang, Y. Fang, Y. Wu, and H. Chen, "Transportation control of double-pendulum cranes with a nonlinear quasi-PID scheme: Design and experiments," *IEEE Trans. Syst., Man, Cybern. Syst.*, to be published, doi: 10.1109/TSMC.2018.2871627.

[61] H. Ouyang, X. Deng, H. Xi, J. Hu, G. Zhang, and L. Mei, "Novel robust controller design for load sway reduction in double-pendulum overhead cranes," *Proc. Inst. Mech. Eng., C, J. Mech. Eng. Sci.*, 2018, doi: 10.1177/0954406218813383.

[62] N. Sun, Y. Wu, Y. Fang, and H. Chen, "Nonlinear antiswing control for crane systems with double-pendulum swing effects and uncertain parameters: Design and experiments," *IEEE Trans. Autom. Sci. Eng.*, vol. 15, no. 3, pp. 1413–1422, Jul. 2018.

[63] N. Sun, Y. Fang, H. Chen, and B. Lu, "Amplitude-saturated nonlinear output feedback antiswing control for underactuated cranes with double-pendulum cargo dynamics," *IEEE Trans. Ind. Electron.*, vol. 64, no. 3, pp. 2135–2146, Mar. 2017.

[64] D. Qian and J. Yi, *Hierarchical Sliding Mode Control for Underactuated Cranes: Design, Analysis and Simulation*. Berlin, Germany: Springer-Verlag, 2016.

HUIMIN OUYANG (M'12) received the B.Eng. degree from the Tianjin Institute of Urban Construction, Tianjin, China, in 2005, the M.Eng. degree from the Nagoya Institute of Technology, Nagoya, Japan, in 2009, and the Ph.D. degree from the Toyohashi University of Technology, Toyohashi, Japan, in 2012.

Since 2013, he has been with the College of Electrical Engineering and Control Science, Nanjing Tech University, Nanjing, China, where he is currently an Assistant Professor. He has published more than 30 papers in journals and international conferences. His major research interests include system control theory and its application to mechatronics.

JIAN WANG received the B.Eng. degree from Nanjing Tech University, Nanjing, China, in 2017, where he is currently pursuing the M.Eng. degree in control engineering. His major research interest includes underactuated rotary crane system control.

GUANGMING ZHANG received the B.Eng. degree from Nanjing Tech University, Nanjing, China, in 1988, and the M.Eng. and Ph.D. degrees from the PLA University of Science and Technology, in 1998 and 2002, respectively.

Since 1998, he has been with the College of Electrical Engineering and Control Science, Nanjing Tech University, where he is currently a Professor. He has published more than 80 papers in journals and international conferences. His major research interest includes advanced control theory for mechatronics.

LEI MEI (M'18) received the B.Eng. degree from the Jiangsu University of Science and Technology, Zhenjiang, China, in 2000, and the Ph.D. degree from the Nanjing University of Aeronautics and Astronautics, in 2009.

Since 2009, he has been with the College of Electrical Engineering and Control Science, Nanjing Tech University, Nanjing, China, where he is currently an Associate professor. He has published more than 20 papers in journals and international conferences. His major research interests include motor design and flywheel energy storage technology and application.

XIN DENG (M'18) received the B.Eng. degree from the Wuhan Chemical Institute of Technology, Wuhan, China, in 2003, and the M.Eng. and Ph.D. degrees from the Huazhong University of Science and Technology, in 2006 and 2010, respectively. In 2010, he joined CSIC 709, where he devoted to wind generation and control system. Since 2013, he has been with the College of Electrical Engineering and Control Science, Nanjing Tech University, Nanjing, China, where he is currently an Assistant Professor. He has published more than 20 papers in journals and international conferences. His major research interests include the sensorless control and design of ac motor.

• • •